scotas
ROBUST FUEL CELLS

SCOTAS-SOFC DELIVERABLE **D3.03**

Report on testing SCO tolerant ST cells towards P=0.4 W/cm^2

DISSEMINATION LEVEL: **PUBLIC**

RESPONSIBLE BENEFICIARY: TOFC

Authors: Compiled by Jeppe Rass-Hansen

Date: Dec 2012

Ver. 01 Covering the project period: 1.10.2010 – 31.10.2012 **Delivered: M27**

1: Introduction

Delivery D3.03 is a short report showing the progress for each ST material towards an electrochemical performance of 0.4 W/cm^2. Only the tests with the best performance results are presented. The LSCT showed the best performance in initial button cell test and was therefore used for the first 5 cell stack see paragraph 4. Results from single cell testing of LSCT are not shown in this report but the 0.4 W/cm^2 have been reached.

2: Anode supported cell test (YST)

2.1: Cell specification

This cell was tested among two other sister-cells at DTU Energy conversion. The cells were produced at Juelich by Dr. Qianli Ma. A similar cell design has been tested by the Karlsruhe Institute of Technology as button-cells, and found to perform satisfactory for the power-output requirements needed.[1] The cell's anode support of YST is ~1000 µm thick, which is thicker than usually tested at DTU Energy conversion. The anode is pre-reduced, therefore the cathode is added later and has to be sintered *in situ*.

The specifications for the cell and the setup during testing are listed in Table 1.

Table 1: Single cell test set-up specification ASC YST

Cell size	5.3 x 5.3 cm^2
Anode current collection	Ni-mesh and Ni plate
Anode support	YST
Anode	YST with 10 mol% excess Ti/YSZ
Anode infiltration	3 wt. % NiO
Electrolyte	YSZ
Cathode current collection	Au mesh and Au plate
Cathode	LSC
Barrier layer	CGO
Sealing and spacers between cell and test-house	Glass bars was used for sealing, and spacers.

2.2: Test conditions and performance data

2.2.1 Initial characterization

Test start-up and reduction: The anode gas-flow during heating was 20l/h of 9% H2 in N2 , and the cathode gas-flow was 50 l/h of air. The cell and cell-house was heated to 950° C. After a sealing and sintering period of 5 hours at 950° C, the temperature was reduced to 900° C. At 900° C the anode was further reduced by a flow of 20 l/h “dry” H2 to the anode for an hour. At “dry” hydrogen, an impedance spectrum (IS) is recorded at OCV, after which the gas flows were increased to: 140l/h of air at the cathode and 24 l/h of humidified (4% H2O) H2 at the anode. IS and iV-curve are measured after a settling period.

After the start-up procedure, leak measurements and characterization was performed. Characterization included iV-curves (down to 650 mV) and IS at 4, 20 and 50 % H2O in H2, between 900 °C and 650 °C at 50 °C intervals; applying a H2 flow of 25 l/h and oxygen flow of 0.5 l/h and 2.5 l/h or a H2 flow of 24 l/h and oxygen flow of 6 l/h; and applying air or oxygen to the cathode at a 140 l/h flow.

2.2.2 Extended characterization

After initial characterization, the temperature of the cell was returned to 850° C and a stability test with 50% H2O in H2 at the anode; air at the cathode and at 0.125 A/cm2 current-load was performed. Subsequently the anode was tested for RedOx stability by slowly changing the anode gas composition from 4% H2O in hydrogen to 20/20/60% O2/H2O/N2. The anode was oxidised for one hour before changing the anode gas to 4% H2O in hydrogen. The anode was reduced for one hour before repeating the cycle. The anode was RedOx-cycled five times this way.

2.3: Results

The initial iV-curves and performance characteristics of the anode supported cell (ASC) with Ni infiltrated YST anode are shown in Figure 1 (left). At the early stages, power outputs above 0.4 W/cm2 were obtained at 900° C. The cell test is conducted despite the inability to fully control the anode chamber gas-composition, as the cell-design in combination with the cell-test setup used is believed to not fully seal the anode from the atmosphere. As the outlet gas-composition, when feeding the cell “dry” or 4% H2O/H2 gas indicate a 30-35% H2O/H2 gas-composition, when the cell is at OCV.

During initial characterization and extended characterization at 850 ° C, the cell-performance degrades, as can be seen in Figure 1 (right). The subsequently RedOx-cycles after is believed to cause the cell crack, drastically degrading the cell-performance (Figure 1 right).

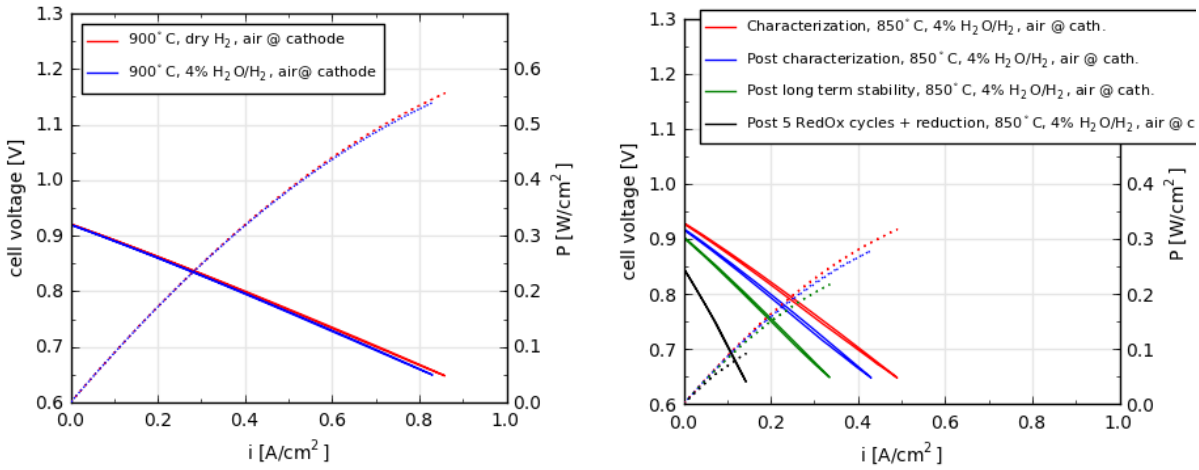

Figure 1: left) iV-curves and power output at the start-up of the cell test with "dry" H_2 (25 l/h, air) flow to the anode and 4% H_2O humidified H_2 to the anode. b) iV-curves and power-outputs during characterization at 850 ° C, after the initial characterization, after long term stability measurement in 50% H_2O/H_2, 0.125 A/cm^2 and after five RedOx-cycles and 24 hours reduction in 4% H_2O/H_2. The iV curves in right) are measured at time period 185, 370, 509 and 573 hours into the experiment. iV-curves are measured in "dry" or 4% H_2O/H_2 by adjusting the anode inlet side gas-composition. pO2 measurements at the outlet indicate a gas-composition of 30-35% H_2O/H_2 when the cell is at OCV and the inlet gas is adjusted to 4% H_2O/H_2. Gas-composition is thus in the 30-35% H_2O/H_2 range when dry or 4% H_2O/H_2 is stated. Air is supplied at 140 l/h to the cathode and the cell temperature is maintained at 850° C.

During extended characterization 850° C the cell voltage was found to degrade at 175 mV/h when the anode gas-composition supplied was 50% H_2O in H_2 at 0.125 A/cm^2 current-load, as can be seen in Figure 2.

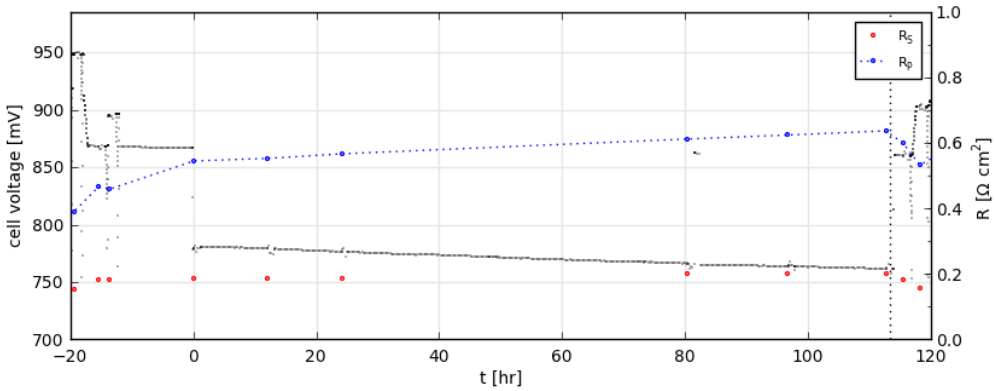

Figure 2: Cell voltages, serial resistances (R_s) and polarization resistances (R_p) derived from impedance spectroscopy during 50% H_2O/H_2 exposure and 0.125 A/cm^2 current-load. The cells R_s and R_p (red and blue dots) increase during testing. The cell voltage degradation during 50% H_2O/H_2 exposure, 0.125 A/cm^2 current-load is 175 mV/h. Air is supplied at 140 l/h to the cathode and the cell temperature is maintained at 850° C.

During high steam exposure and current load (50% H_2O in H_2 at 0.125 A/cm^2), both serial resistance (R_s) and polarization resistance (R_p) increase, indicating both decreased conductivity of the backbone and decreased stability of the Ni infiltrate nano-particles. The subsequent five RedOx-cycles (not shown) cause the cell to crack, as the cell temperature increases by 7° C and R_s and R_p increase dramatically.

2.4: Conclusions

The Pre-reduced YST ASC with Ni-infiltrate exhibits an excellent power-output at the beginning of the test at 900° C, but decreases significantly when lowering the temperature to 850° C. During initial characterization and later during extended characterization of the cell, the performance decreases. After five RedOx-cycles of the anode causes the cell to crack, thus degrading the performance considerably. The cell performance stability and test-setup improvements to confidently test these ASC are main issues at the moment.

3: Electrolyte supported cell test (STN94)

3.1: Cell specification

This cell was tested after the addition of platinum paste to the anode surface to act as a current collecting layer (CCL). Pt paste as CCL on the anode was used during anode screening, and Hexis performed a button-cell test with Pt paste as a current collector, which exhibited better performance by lowering the serial resistance measured. The cell is an electrolyte supported cell, thus the electrolyte is ~200 µm thick.

The specifications for the cell and the setup during testing are listed in Table 2.

Table 2: Single cell test set-up specification ESC STN94

Cell size	5.3 x 5.3 cm^2
Anode current collection	Pt paste as CCL, Ni-mesh and Ni plate
Anode backbone	STN94 with 10% vol. 8YSZ
Anode infiltration	3 M CGO with 10 wt. % Ni
Electrolyte	YSZ
Cathode current collection	Au mesh and Au plate
Cathode	LSM/YSZ
Cathode contact layer	LSM
Sealing and spacers between cell and test-house	Glass was used as sealant, and metal frames used as spacers.

3.2: Test conditions and performance data

3.2.1 Test start-up and reduction

The anode gas-flow during heating was 20l/h of 9% H2 in N2 , and the cathode gas-flow was 50 l/h of air. The cell and cell-setup was heated to 850° C. After a sealing and reduction period of 2 hours at 850° C, the anode was further reduced by a flow of 20 l/h “dry” H2 to the anode. After an hour at “dry” hydrogen, an impedance spectrum (IS) is recorded at OCV, after which the gas flows are increased to: 140 l/h of air at the cathode and 24 l/h of humidified (4% H2O) H2 at the anode. IS and iV-curve are measured sequentially.

After the start-up procedure, leak measurements and characterization was performed.

3.2.2 Initial Characterization

iV-curves (down to 650 mV) and IS at 4, 20 and 50 % H2O in H2, between 850 °C and 650 °C at 50 °C intervals; applying a H2 flow of 24 l/h through a bubble-flask with water, a H2 flow of 25 l/h and oxygen flow of 2.5 l/h or a H2 flow of 24 l/h and oxygen flow of 6 l/h; and applying air or oxygen to the cathode at a 140 l/h flow. IS are measured at OCV.

3.2.3 Extended characterization

After initial characterization, the temperature of the cell was raised again to 850° C and RedOx cycled by slowly changing the anode gas composition from 4% H2O in hydrogen to 20/20/60 % O2/H2O/N2. The anode was oxidised for one hour before changing the anode gas back to 4% H2O in hydrogen, where the anode was kept for at least 24 hours for reduction.
The cell was subsequently tested under internal methane reforming (IR) conditions (gas composition: 30/60/10 CH4/H2O/H2) with flows and current-load adjusted to 60 % fuel-utilization (0.27 A/cm2, 0.7/0.7/1.655 l/h CH4/O2/H2) an additional test at equivalent conditions with an addition of 2 ppm H2S was performed subsequently. A RedOx cycle of the anode was performed in between tests.

3.3: Results

The initial iV-curves and performance characteristics of the cell with a Ni/CGO infiltrated STN94/8YSZ anode are shown in Figure 3a. At the early stages, power outputs above 0.4 W/cm2 were obtained. After initial characterization of the cell for less than 100 hours, and a RedOx cycle of the anode, the power-output has decreased significantly, as can be seen in Figure 3b. Subsequent reduction of the anode in 4% H2O/H2 for 24 hours at 850° C does not improve the anode performance, as the power output is further decreased.

Running the cell under methane internal reforming conditions, and 60 % fuel utilization, degrades the cell rapidly, as the cell potential drops from 650 mV to 450 mV in less than 12 hours. After Redox-cycling the anode in technical humidified air, the iV-curve and power-output looks similar to what was measured before IR(see Figure 3b), yet upon returning the cell to 60% fuel utilization under IR, the cell potential drops instantaneously to 450 mV. This is expected due to the absence of Ni to catalyse the water-gas-shift reaction.

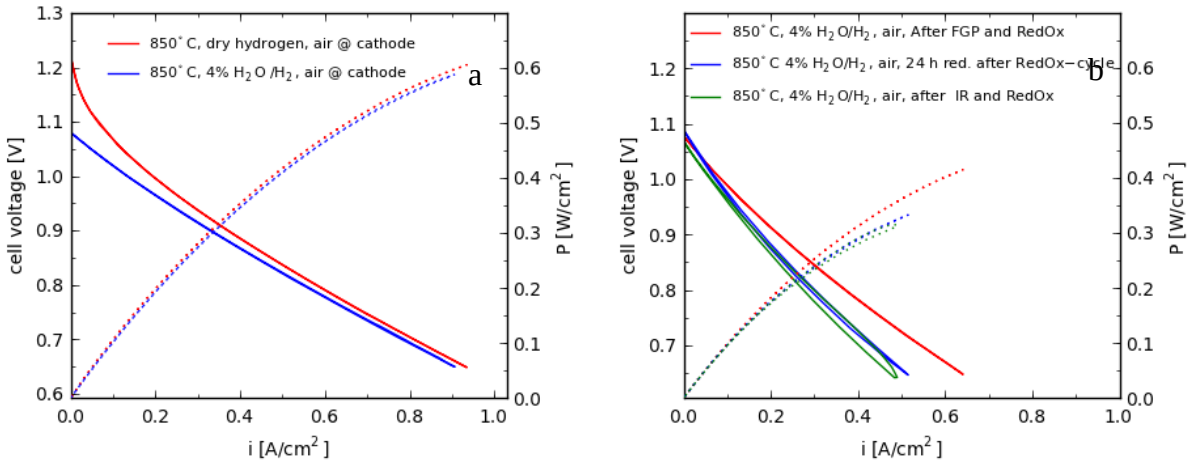

Figure 3: a) iV-curves and power output at the start-up of the cell test with "dry" H_2 (25 l/h, air) flow to the anode and 4% H_2O humidified H_2 to the anode. b) iV-curves and power-outputs after the initial RedOx following the cell characterization, 24 hours later after reduction in 4% H_2O/H_2 and after IR conditions, 60% fuel utilization and a subsequent second RedOx cycle. The iV curves in b) are measured at time period 120, 145 and 177 hours into the experiment. iV-curves are measured in 4% H_2O/H_2 to the anode with air at the cathode, unless stated otherwise.

3.4: Conclusions:

The cell with STN94/8YSZ anode exhibits an excellent power-output at the beginning of the test, but decreases significantly after initial characterization. A RedOx of the anode slightly improves power-output. The cell-performance degrades rapidly under internal reforming conditions, as expected. RedOx cycling the anode increases the cell performance slightly, but the cell performance degraded instantaneously under internal reforming conditions. The degradation of the power-output over time is still considered a focal issue, and connected to the stability of the nano-infiltrates.

4: Electrolyte supported cells stack test (LSCT)

4.1: Cell specification

In order to benchmark the cells with LSCT anodes from University of St. Andrews a 5 cells test was built up in the Hexis lab. This type of cell showed a reasonable performance on button cell level. The cell geometries and the materials used are listed in Table 3.

Table 3: cell and stack parameters

Cell size	D=120mm, Hexis design
Anode current collection	Ni-mesh
Anode	LSCT+Ni+Ce
Electrolyte	6 ScSZ, 160 µm
Cathode	LSM/YSZ
Cathode contact layer	LSM
Interconnect	CFY (Plansee)

4.2: Test conditions and performance data

Test conditions: The stack was operated at 900°C, with partially oxidized natural gas (CPOx, 4 g/h per cell) and 200 mA/cm2. Current-Potential (IV) characteristics and Electrical Impedance Spectroscopy (EIS) were performed subsequently. The same testing conditions are usually used for the Hexis standard cells. In order to test the sulphur stability of the LSCT anodes, the desulphurizer was by-passed two times during the experiment for approximately 10 hours.
Furthermore, 2 redox-cycles were carried out. Therefore the gas was shut down abruptly at 900°C. The anode is oxidized for 2 hours by back diffusion of air (open stack design). In nickel based anodes the oxidation process is completed within minutes in this temperature range.
After the oxidation, the cell is operated at OCV for about 6 hours before polarizing the stack again.

4.3: Results

The IV and performance characteristics of the cell with the LSCT anode is shown in Figure 4 in comparison with a Hexis standard cell under the same experimental conditions. Both data were recorded at the beginning of the experiment. The cathode was the same for all cells. It can be seen that the Hexis standard cell is performing slightly better under these experimental conditions. However, the performance of the cell having a LSCT anode is considered to be reasonable at that state of the project.

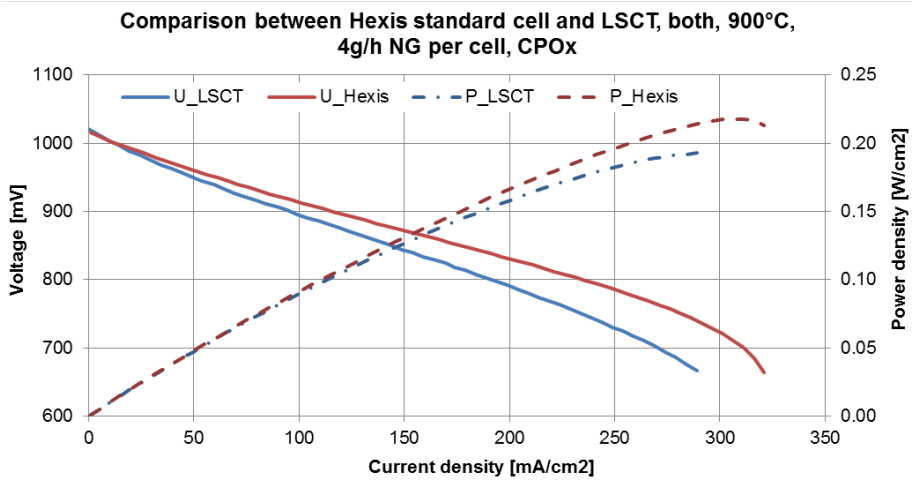

Figure 4: IV and performance characteristic of the cell with the LSCT anode in comparison with the Hexis cell (start of experiment). A fuel utilisation of 80% is reached around 250 mA/cm2.

A comparison of the stack potential over time between a stack with LSCT anodes and the Hexis standard is shown in Figure 5. It can be seen that the degradation is significantly faster already in the first 200 hours. When bypassing the desulphurizer the stack showed even higher degradation (not shown here).

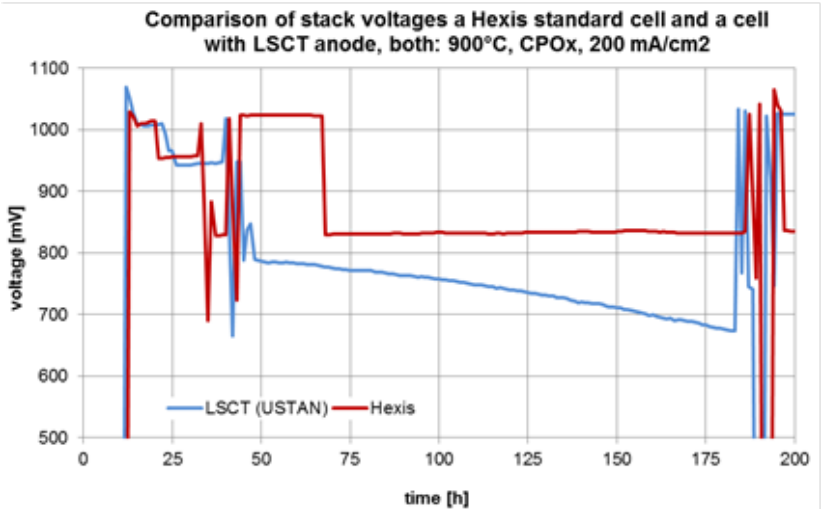

Figure 5: Comparison of the stack potential over time between cells with the LSCT anodes and Hexis standard cells

4.4: Conclusion:

The cells with LSCT anodes showed a reasonable performance at the beginning of the experiment but heavy degradation over time. Therefore degradation is considered to be the most critical challenge at the moment.

5: Conclusion

The goal in this delivery report is to show performance of 0.4 W/cm^2. This has been shown on both ASC (YST cell from Jülich) and ESC (STN94 cell from DTU). Early tests from button cells indicated that ESC with LSCT from USTAN had the highest performance of the different strontium titanates. Therefore these cells were used in the first 5 cell stack tested at Hexis. There is, however, quite a difference from testing in a cell setup with very low fuel utilisation and a stack test with a much higher fuel utilisation; consequently it should not be expected to achieve similar performance (0.4 W/cm^2) in stack testing. Nevertheless, as starting performance the LSCT showed comparable results to the standard Hexis cells indicating the possibilities of the ST.

In conclusion all three types of ST have shown good starting performance in the expected range, but also it is clear that all materials degrade too fast so far. One important focus area should therefore be the stability of the cells and primarily on impregnates used. Another focus area is to test with relevant testing conditions. The ST anodes should be more sulphur, carbon and redox stable than standard nickel based anodes, thus it is important that this is shown in coming test, and that the ST cells also prove a high power output on sulphur and carbon containing fuels.

References

1. Q. Ma, F. Tietz, A. Leonide, and E. Ivers-Tiffée, *Journal of Power Sources*, **196**, 7308–7312 (2011) http://dx.doi.org/10.1016/j.jpowsour.2010.07.094.